THE JOURNAL OF COMPARATIVE NEUROLOGY 499:231–243 (2006)

Differential Synaptology of vGluT2-Containing Thalamostriatal Afferents Between the Patch and Matrix Compartments in Rats

DINESH V. RAJU,[1] DEEP J. SHAH,[2] TERRENCE M. WRIGHT,[3] RANDY A. HALL,[4] AND YOLAND SMITH[1,5]*

[1]Yerkes National Primate Research Center, Emory University, Atlanta, Georgia 30322
[2]University of Georgia, Athens, Georgia 30609
[3]Department of Biology, Emory University, Atlanta, Georgia 30322
[4]Department of Pharmacology, Emory University, Atlanta, Georgia 30322
[5]Department of Neurology, Emory University, Atlanta, Georgia 30322

ABSTRACT

The striatum is divided into two compartments named the *patch* (or striosome) and the *matrix*. Although these two compartments can be differentiated by their neurochemical content or afferent and efferent projections, the synaptology of inputs to these striatal regions remains poorly characterized. By using the vesicular glutamate transporters vGluT1 and vGluT2, as markers of corticostriatal and thalamostriatal projections, respectively, we demonstrate a differential pattern of synaptic connections of these two pathways between the patch and the matrix compartments. We also demonstrate that the majority of vGluT2-immunolabeled axon terminals form axospinous synapses, suggesting that thalamic afferents, like corticostriatal inputs, terminate preferentially onto spines in the striatum. Within both compartments, more than 90% of vGluT1-containing terminals formed axospinous synapses, whereas 87% of vGluT2-positive terminals within the patch innervated dendritic spines, but only 55% did so in the matrix. To characterize further the source of thalamic inputs that could account for the increase in axodendritic synapses in the matrix, we undertook an electron microscopic analysis of the synaptology of thalamostriatal afferents to the matrix compartments from specific intralaminar, midline, relay, and associative thalamic nuclei in rats. Approximately 95% of PHA-L-labeled terminals from the central lateral, midline, mediodorsal, lateral dorsal, anteroventral, and ventral anterior/ventral lateral nuclei formed axospinous synapses, a pattern reminiscent of corticostriatal afferents but strikingly different from thalamostriatal projections arising from the parafascicular nucleus (PF), which terminated onto dendritic shafts. These findings provide the first evidence for a differential pattern of synaptic organization of thalamostriatal glutamatergic inputs to the patch and matrix compartments. Furthermore, they demonstrate that the PF is the sole source of significant axodendritic thalamic inputs to striatal projection neurons. These observations pave the way for understanding differential regulatory mechanisms of striatal outflow from the patch and matrix compartments by thalamostriatal afferents. J. Comp. Neurol. 499:231–243, 2006.

Indexing terms: immunocytochemistry; vGluT1; vGluT2; thalamus; striatum

Grant sponsor: National Institutes of Health (to Y.S., R.A.H.); Grant sponsor: National Research Service Award (to D.V.R.); Grant sponsor: National Institutes of Health; Grant number: RR 00165 (to Yerkes National Primate Research Center); Grant sponsor: W.M. Keck Foundation (to R.A.H.).

*Correspondence to: Yoland Smith, PhD, Yerkes National Primate Research Center, Emory University, 954 Gatewood Road NE, Atlanta, GA 30322. E-mail: ysmit01@emory.edu

Received 23 January 2006; Revised 28 April 2006; Accepted 20 May 2006
DOI 10.1002/cne.21099
Published online in Wiley InterScience (www.interscience.wiley.com).

The medium spiny neuron (MSN) is the primary projection neuron of the striatum and serves as a locus for glutamatergic inputs from most areas of the neocortex and various thalamic nuclei (Somogyi et al., 1981; Berendse and Groenewegen, 1990; Kawaguchi et al., 1990; Kawaguchi, 1997). It is well established that corticostriatal afferents innervate the head of dendritic spines of MSNs and, to a lesser degree, dendritic shafts of γ-aminobutyric acid (GABA)-ergic interneurons (Dube et al., 1988; Lapper et al., 1992; Sidibe and Smith, 1999). However, most of our understanding of the synaptic microcircuitry of the thalamostriatal system comes from extensive studies of the projections from the caudal intralaminar nuclei, namely, the centromedian (CM)/parafascicular (PF) complex (Dube et al., 1988; Meredith and Wouterlood, 1990; Lapper and Bolam, 1992; Sadikot et al., 1992b; Smith et al., 2004). In both rats and monkeys, CM and PF projections mainly form asymmetric synapses onto dendritic shafts of MSNs and interneurons (Lapper and Bolam, 1992; Sidibe and Smith, 1999). These results suggest that corticostriatal and thalamostriatal afferents form synapses preferentially onto dendritic spines and shafts, respectively. However, recent work using vesicular glutamate transporter 2 (vGluT2) as a selective marker of thalamic inputs to the dorsal striatum showed that thalamostriatal afferents form primarily axospinous synapses in rat (Lacey et al., 2005; Raju and Smith, 2005), raising the interesting possibility that the PF may be unique in forming primarily axodendritic synapses onto MSNs.

Although MSNs appear to be homogenously distributed in the striatum, these neurons are strictly segregated into two neurochemically defined striatal compartments, namely, the patch (or striosome) and matrix (Graybiel et al., 1981; Herkenham and Pert, 1981). Projections from sensorimotor cortices and most thalamic nuclei innervate preferentially the matrix (Herkenham and Pert, 1981; Ragsdale and Graybiel, 1981, 1991; Gerfen, 1984, 1989, 1992; Berendse and Groenewegen, 1990; Sadikot et al., 1992b), whereas corticostriatal afferents from limbic and prefrontal association cortices, as well as thalamic inputs from the paraventricular (PV) and rhomboid nuclei, terminate quite selectively within patches (Gerfen, 1984, 1989; Berendse and Groenewegen, 1990; Eblen and Graybiel, 1995; Wang and Pickel, 1998). Although various markers and projections have been specifically associated with the patch or matrix compartments, very little is known about the differential synaptology of these two striatal compartments. A clearer understanding of the specific connectivity that underlies the regulation of neurons in these regions is a prerequisite for a deeper knowledge of the functional significance of this anatomical organization. Furthermore, recent findings showing that an imbalanced activity between the patch and the matrix compartments leads to repetitive motor behaviors (Canales and Graybiel, 2000) and that selective neurodegeneration of patches occurs in X-linked progressive dystonia-parkinsonism (Goto et al., 2005) highlight the importance of better understanding the basic mechanisms that regulate the functional activity in these two striatal compartments. Therefore, we undertook a detailed electron microscopic analysis of glutamatergic inputs to the striatum that aimed at achieving the following goals: 1) compare the synaptic microcircuitry of glutamatergic inputs to the patch and matrix compartments by using vGluT1 and vGluT2 as specific markers of the corticostriatal and thalamostriatal projections, respectively, and 2) characterize the synaptic organization of thalamic projections from various intralaminar and nonintralaminar nuclei to the rat striatum, by using anterograde tract tracing methods.

Abbreviations

AM	anteromedial nucleus
AV	anteroventral nucleus
CL	central lateral nucleus
CeM	central medial nucleus
CM	centromedian nucleus
Hb	habenula
IMD	intermediodorsal nucleus
LD	lateral dorsal nucleus
LDVL	lateral dorsal nucleus, ventrolateral part?
LDDM	lateral dorsal nucleus, dorsomedial part
LP	lateral posterior nucleus
MD	mediodorsal nucleus
M1	primary motor cortex
M2	secondary motor cortex
PC	paracentral nucleus
PF	parafasicular nucleus
PV	paraventricular nucleus
Po	posterior thalamic nucleus
RT	reticular nucleus
VA	ventral anterior nucleus
VL	ventral lateral nucleus
VP	ventral posterior nucleus
VPL	ventral posterior lateral nucleus
VPM	ventral posterior medial nucleus

MATERIALS AND METHODS

Synthesis and specificity of vGluT1 antibodies

A new anti-vGluT1 antiserum was generated. To generate these antibodies, a peptide from the COOH terminus of the rat vesicular glutamate transporter 1 (rvGluT1), corresponding to amino acids 543–560 (cATHSTVQPPRPPPPVRDY), was synthesized. The epitope is absolutely conserved in the mouse vGluT1 sequence and has one site of divergence in the human sequence (italicized above). A cysteine was added to the peptide to aid its conjugation to the protein carrier keyhole limpet hemocyanin (KLH; Pierce, Rockford, IL). Antisera were obtained from rabbits (Covance) immunized with the conjugated peptide, and the IgG fraction was recovered by ammonium sulfate precipitation as follows. Sera were first treated with 25% ammonium sulfate to remove any proteins that might precipitate at low ionic concentrations and incubated with stirring overnight at 4°C. After a 3,000*g* 30-minute spin, the supernatant was removed and transferred to a clean tube. Ammonium sulfate was added to a final concentration of 50% saturation. After another overnight incubation at 4°C, the IgG fraction was isolated in the pellet by centrifugation at 3,000*g* for 30 minutes. The pellet was resuspended in PBS and dialyzed overnight with three buffer changes.

Western immunoblots

Fresh frozen brain tissue from two Sprague-Dawley rats (Charles River Laboratories, Wilmington, MA) was homogenized, resolved by SDS-PAGE, and subjected to Western blot analysis with anti-vGluT1 (0.2 μg/ml) anti-

TABLE 1. Sources and Immunogens of Antibodies

Antibody (immunocytochemistry concentration)	Vendor	Catalog No.	Lot No.	Immunogen	Immunizing species
vGluT1 (0.2 μg/ml)	Mab Technologies (Atlanta, GA)	VGT1-3	GA061-031003	Rat aa 543-560	Rabbit
vGluT2 (0.2 μg/ml)	Chemicon (Temecula, CA)	AB5907	22050779	Rat aa 565-582	Guineapig
μ-OR (0.1 μg/ml)	Chemicon	AB5511	24121675	Rat aa 384-398	Rabbit
PHA-L (0.2 μg/ml)	Vector (Burlingame, CA)	AS-2300	Q0205	—	Rabbit

bodies. Immunoreactive bands were detected with the enhanced chemiluminescence detection system (Pierce) with horseradish peroxidase-conjugated goat anti-rabbit secondary antibody (1:4,000; Amersham Biosciences, Little Chalfont, United Kingdom). Preadsorbtion of primary antibody with synthetic peptide (0.2–0.4 μg/ml) overnight at 4°C abolished immunoreactivity, whereas preadsorbtion with a similar but nonidentical peptide preserved immunoreactivity.

Animals and perfusion fixation

In total, 26 adult male (body weight 285–315 g) Sprague-Dawley rats (Charles River Laboratories) were used in this study. The experiments were performed according to the National Institutes of Health guidelines for the care and use of laboratory animals. All efforts were made to minimize animal suffering and reduce the number of animals used.

In all cases, animals were deeply anesthetized with ketamine (60–100 mg/kg) and dormitor (0.1 mg/kg) and transcardially perfused with 40–50 ml cold Ringer's solution, followed by 400 ml of fixative containing a mixture of 4% paraformaldehyde and 0.5% glutaraldehyde in phosphate buffer (0.1 M, pH 7.4). After fixative perfusion, the brains were taken from the skull and postfixed in 4% paraformaldehyde for 6–8 hours. Tissue sections (60 μm thick) were cut with a Vibratome, collected in cold phosphate-buffered saline (PBS; 0.01 M, pH 7.4), and treated with sodium borohydride (1% in PBS) for 20 minutes.

Primary antibodies

The commercial sources and immunogen amino acid sequences used to generate polyclonal antibodies against vGluT1, vGluT2, μ-opioid receptor (μ-OR), and *Phaseolus vulgaris* leucoagglutinin (PHA-L) used in this study are shown in Table 1. Western blot analysis of the anti-vGluT1 antibodies identified single bands at ~60 kDa (Fig. 1A), as predicted for the vGluT1 protein (Montana et al., 2004). Preadsorbtion with the immunogenic peptide abolished labeling, whereas preadsorbtion with similar, but heterologous, peptide maintained immunoreactivity (Montana et al., 2004; Raju and Smith, 2005). Identical preadsorbtion controls were performed with the anti-vGluT1 antibody on rat striatal tissue (Fig. 1B–E). The anti-vGluT1 antibody immunolabeled the neuropil within the rat striatum, but the labeling was completely abolished when the antibodies were preadsorbed with the vGluT1, but not vGluT2, control peptide (Fig. 1C,D). The specificity of the vGluT2 antiserum was carefully tested by immunoblotting and immunocytochemistry in a previous study (Montana et al., 2004).

The pattern of μ-OR immunolabeling shown in this study is similar to that reported in several previous studies (Graybiel et al., 1981; Desban et al., 1989, 1993). Omission of the primary antibody in control experiments abolished immunolabeling.

Similarly, omission of PHA-L antibodies from incubation solution led to a complete lack of immunoreactive fibers and terminals in striatal tissue ipsilateral to the thalamic injections. Furthermore, in cases involving unilateral thalamic injections of PHA-L, the contralateral striatum was devoid of immunolabeling.

Localization of vGluT1 and vGluT2 in the patch and matrix compartments

To examine the distribution of vGluT1 and vGluT2 in the striatal patch or matrix compartments of the striatum, one series of three serially cut sections was obtained from each of the four animals used in these experiments. The second of the three sections was stained for μ-OR at the light microscopic level, whereas the first and third sections were stained for either vGluT1 or vGluT2 and prepared for electron microscopic observation. Once placed in sequential order, the section stained for μ-OR was used as a marker to help cut tissue blocks from the vGluT1- or vGluT2-immunostained sections that corresponded to either the densely or the lightly stained patch and matrix compartments, respectively. All blocks were taken from the dorsal striatum. For light and electron microscopic examination, tissue sections were processed using the ABC immunoperoxidase method (Hsu et al., 1981a,b).

Light microscopic observation of μ-OR. All incubations were performed at room temperature. After blocking for 1 hour in a PBS solution containing 1% normal goat serum, 1% bovine serum albumin (BSA; Sigma, St. Louis, MO), and 0.3% Triton X-100, tissue sections were rinsed in PBS (3 × 10 minutes) and then incubated for 12–16 hours with rabbit anti-μ-OR primary antibody in solution identical to the blocking solution. After three rinses in PBS, the tissue was incubated with biotinylated goat anti-rabbit secondary antibodies (5 μg/ml; Vector, Burlingame, CA) in the same solution as above for 90 minutes. After being washed with PBS, the tissue was then incubated with avidin-biotin-peroxidase complex (1% ABC; Vectastain Standard Kit; Vector) in a PBS solution containing 1% BSA and 0.3% Triton X-100 for 90 minutes. After two washes in PBS, the tissue was washed in a Tris buffer (0.05 M, pH 7.6) and then placed in Tris solution containing the chromogen 3,3′-diaminobenzidine tetrahydrochloride (DAB; 0.025%; Sigma), 0.01 M imidazole (Fisher Scientific, Norcross, GA), and hydrogen peroxide (0.006%) for 10 minutes. The DAB reaction was terminated with several rinses in PBS. The sections were then mounted onto gelatin-coated slides and dehydrated, and a coverslip was applied with Permount.

Electron microscopic localization of vGluT1 and vGluT2 immunoreactivity. The sections were placed in a cryoprotectant solution (PB; 0.05 M, pH 7.4, containing 25% sucrose and 10% glycerol) for 20 minutes, frozen at

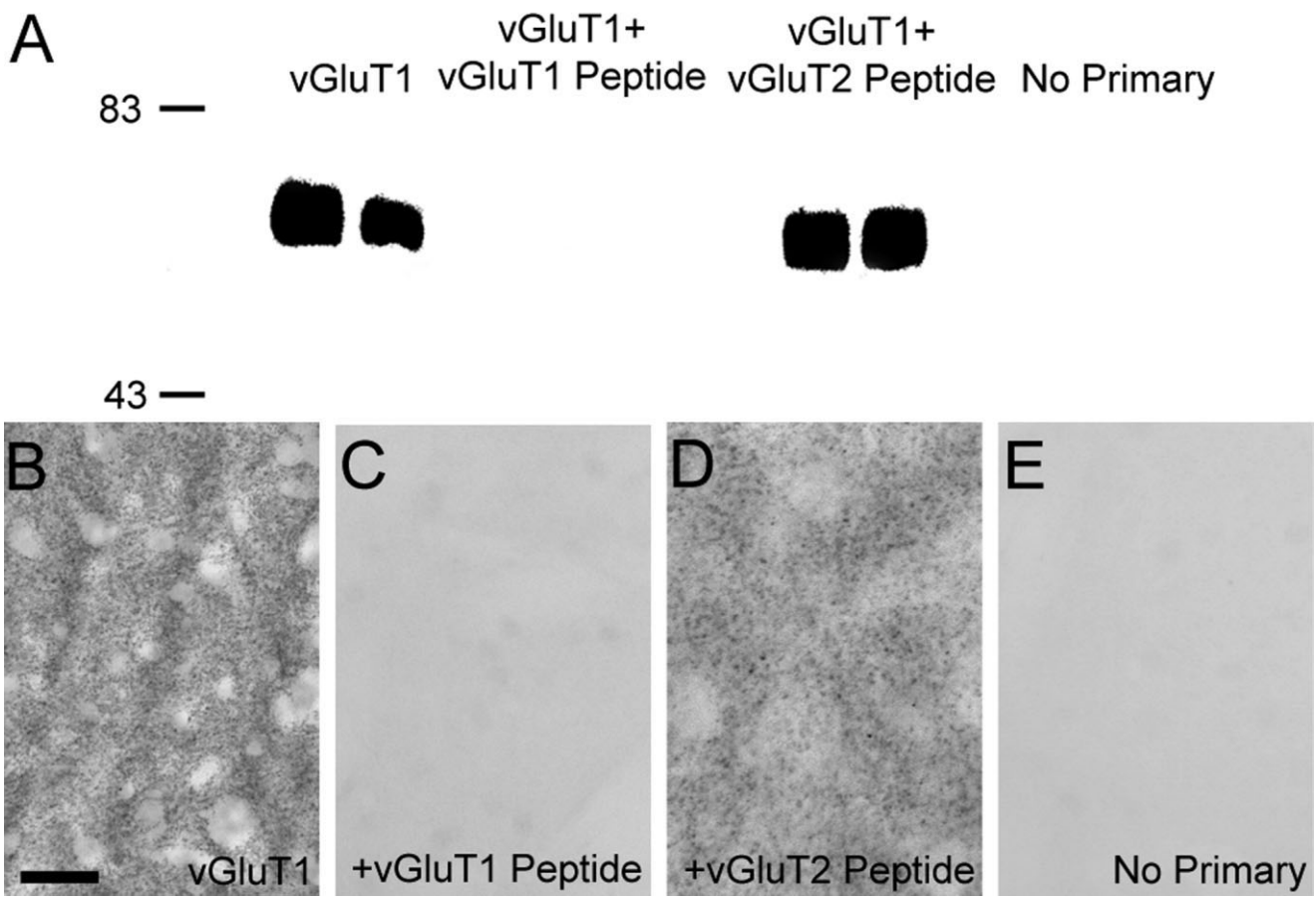

Fig. 1. vGluT1 antibody specificity. **A:** Western blot analysis demonstrating the specificity of antibodies against vGluT1. Anti-vGluT1 antibodies detected proteins of ~60 kDa corresponding to the molecular weight predicted for the vGluT1 protein in striatal tissue from two different rats. The immunoreactivity is completely abolished when antibodies are omitted (no primary) or preadsorbed with the synthetic vGluT1 peptide prior to immunoblotting, but it is preserved when anti-vGluT1 antibody is preadsorbed with synthetic vGluT2 peptide. **B–E:** Light microscopic examination of rat striatal tissue stained with anti-vGluT1 antibodies demonstrates neuropil immunoreactivity (B), which is abolished when antibodies are preadsorbed with the synthetic peptide (C). Immunoreactivity is preserved when antibodies are preadsorbed with the vGluT2 peptide (D). Immunostaining of striatal tissue without primary antibodies is shown for reference (E). Molecular weight standards are indicated on the left (in kDa). Scale = 50 μm.

−80°C for 20 minutes, thawed, and returned to a graded series of cryoprotectant (100%, 70%, 50%, 30%) diluted in PBS. They were then washed in PBS before being processed for immunocytochemistry.

The sections were preincubated for 1 hour at room temperature in a PBS solution containing 1% normal goat serum and 1% BSA and then incubated for 48 hours with rabbit anti-vGluT1 or guinea pig anti-vGluT2 primary antibody diluted in the preincubation solution. After three rinses in PBS, the tissue was incubated with biotinylated goat anti-guinea pig or goat anti-rabbit secondary antibodies (5 μg/ml; Vector) in the same solution as described above for 90 minutes. After washing with PBS, the tissue was then incubated with ABC (1%; Vector) in a PBS solution containing 1% BSA for 90 minutes at room temperature. Subsequent steps for the DAB reaction were identical to those described above.

After immunostaining, sections were washed in PB (0.1 M, pH 7.4) and postfixed in osmium tetroxide (1% in PB). This was followed by rinses in PB (0.1 M, pH 7.4) and dehydration in a graded series of ethanol (50%, 70%, 90%, 100%) and propylene oxide. Uranyl acetate (1%) was added to the 70% ethanol to improve the contrast in the electron microscope. The sections were then embedded in resin (Durcupan ACM; Fluka, Fort Washington, PA), mounted on microscope slides, and placed in an oven for 48 hours at 60°C. Areas of interest were selected, cut from the slides, and glued on the top of resin blocks. Ultrathin sections were obtained on an ultramicrotome (Leica Ultracut T2), collected onto Pioloform-coated single-slot copper grids, stained with lead citrate (Reynolds, 1963), and examined with an electron microscope (Zeiss EM 10C). The electron micrographs were acquired with a CCD camera (DualView 300W; Gatan, Pleasanton, CA) and Digital Micrograph software (version 3.8.1; Gatan). For all images taken, the observer was blinded concerning where, either the patch or the matrix, the block was cut. Some digitally acquired micrographs were adjusted only for brightness and contrast, with the image resolution kept constant, with either Digital Micrograph or Photoshop software (version 7.0; Adobe Systems, Inc., San Jose, CA) to optimize the quality of the images for analysis.

TABLE 2. Number of Animals, Hemispheres, and Blocks and Total Surface Area Examined in the Different Experimental Cases

	Animals	Hemispheres	Blocks	Surface area (μm^2)
vGluT1 patch	4	4	4	2,270
vGluT2 patch	4	4	4	2,244
vGluT1 matrix	4	4	4	2,270
vGluT2 matrix	4	4	4	2,244
M1	3	3	3	1,590
PF	3	3	3	1,601
CL	3	3	3	1,313
Midline	3	4	4	1,562
MD	3	5	6	1,210
LD	2	2	2	1,413
AV	3	3	4	370
VA/VL	3	3	3	1,228

Anterograde tract tracing experiments

All rats received either a unilateral or bilateral iontophoretic injection of the anterograde tracer PHA-L in the thalamus or primary motor cortex. After being anesthetized with ketamine (60–100 mg/kg) and dormitor (0.1 mg/kg), the rats were fixed in a stereotaxic frame (Knopf). A glass micropipette (20–35 μm tip diameter), containing PHA-L (2.5% in 0.1 M, pH 8.0, phosphate buffer; Vector) was placed in the M1, PF, VA/VL, AV, LD, MD, CL, or midline nuclei (as per coordinates of Paxinos and Watson, 1998), and iontophoretic delivery of tracer was performed with a 7-μA positive current for 20 minutes via a 7-seconds-on/7-seconds-off cycle. The paraventricular and intermediodorsal nuclei were grouped as the midline nuclei. After the appropriate survival period (6–8 days), the rats were perfusion fixed as described above. The brains were serially cut (60-μm-thick sections) and reacted with sodium borohydride.

To reveal the injected and transported PHA-L, every sixth section of each rat brain was processed for light microscopy as described above. Briefly, the sections were incubated with rabbit anti-PHA-L antibodies and then with biotinylated secondary goat anti-rabbit IgGs. The PHA-L was revealed by using the ABC method and DAB as the chromogen. To determine the extent of the thalamic injection sites, several sections preceding and following the core of the injection track were processed to reveal PHA-L and counterstained with cresyl violet before coverslipping. For electron microscopy, tissue sections were selected, immunostained for PHA-L, and prepared for electron microscopy as described above. Blocks of tissue from areas containing dense plexi of anterogradely labeled fibers were selected and cut into ultrathin sections for electron microscopic observation.

Analysis of material

Immunoperoxidase labeling. To minimize false negatives, only ultrathin sections from the most superficial sections of blocks were scanned at ×25,000, and all immunoreactive axon terminals forming a clear synapse were photographed. The number of blocks and total surface of tissue examined in each experimental group are given in Table 2. The labeled elements were categorized as axon terminals forming asymmetric synapses onto either dendrites or spines, based on ultrastructural criteria defined by Peters et al. (1991). Their relative proportion was calculated and expressed as a percentage of total labeled axon terminals expressing vGluT1, vGluT2, or PHA-L from individual thalamic nuclei. Statistical differences in the pattern of distribution of the vGluTs and immunolabeled thalamostriatal axon terminals were assessed with Kruskal-Wallis one-way ANOVA on ranks and subsequent Dunn's post hoc analysis (SigmaStat 3.0). Statistical significance was considered at $P < 0.05$.

Injection sites and striatal projections. The thalamic injection sites were digitally photographed at a magnification of ×8 with a light microscope (Leica 420) and an RT Spot camera. The cresyl violet-stained sections were utilized to delineate neighboring thalamic nuclei. Striatal immunolabeling at the light microscopic level was digitally photographed at a magnification of ×20 with a Leica DC 500 digital camera.

RESULTS

Differential localization of vGluT1 and vGluT2 in the patch and matrix compartments

To examine the subcellular distribution of the vGluTs in the patch and matrix compartments of the striatum, the ABC electron microscopy immunoperoxidase method was utilized. Initially, one series of three serial sections of dorsal striatum from each animal was processed to reveal vGluT1, μ-OR, or vGluT2. The first and third sections were immunolabeled for vGluT1 or vGluT2, respectively, and processed for electron microscopic observations, whereas the middle section was immunolabeled for μ-OR to identify intensely labeled patches within the dorsal striatum. Once aligned in order, the μ-OR-immunostained section was used to identify the patch and matrix regions in adjacent vGluT1- and vGluT2-immunostained sections (Fig. 2A–C).

In the electron microscope, the DAB-labeled antigenic sites were recognized by the presence of amorphous electron-dense deposit (Fig. 2A,B). Immunolabeling was restricted exclusively to axon terminals and unmyelinated axons containing synaptic vesicles. In both the patch and the matrix compartments, more than 90% of the postsynaptic targets of vGluT1-immunolabeled terminals were dendritic spines, with no significant differences between the two compartments (Fig. 3). In contrast, there was a striking difference in the pattern of synaptic connectivity of vGluT2-immunoreactive terminals between the patch and the matrix compartments. In the patch compartment, the distribution of vGluT2 immunoreactivity was nearly identical to that of vGluT1; that is, almost 90% of labeled terminal boutons formed axospinous synapses. However, in the matrix compartment, vGluT2-immunolabeled axon terminals formed asymmetric synapses nearly equally onto dendritic spines and shafts ($P > 0.05$).

Synaptic organization of specific thalamic inputs to the striatum

To characterize further the thalamic sources of axospinous vs. axodendritic glutamatergic synapses in the striatum, we used PHA-L to label anterogradely specific thalamic inputs from a large variety of relay, associative, and intralaminar thalamic nuclei to the rat striatum. For purposes of comparison with the corticostriatal system, PHA-L injections were also made in the primary motor cortex (M1).

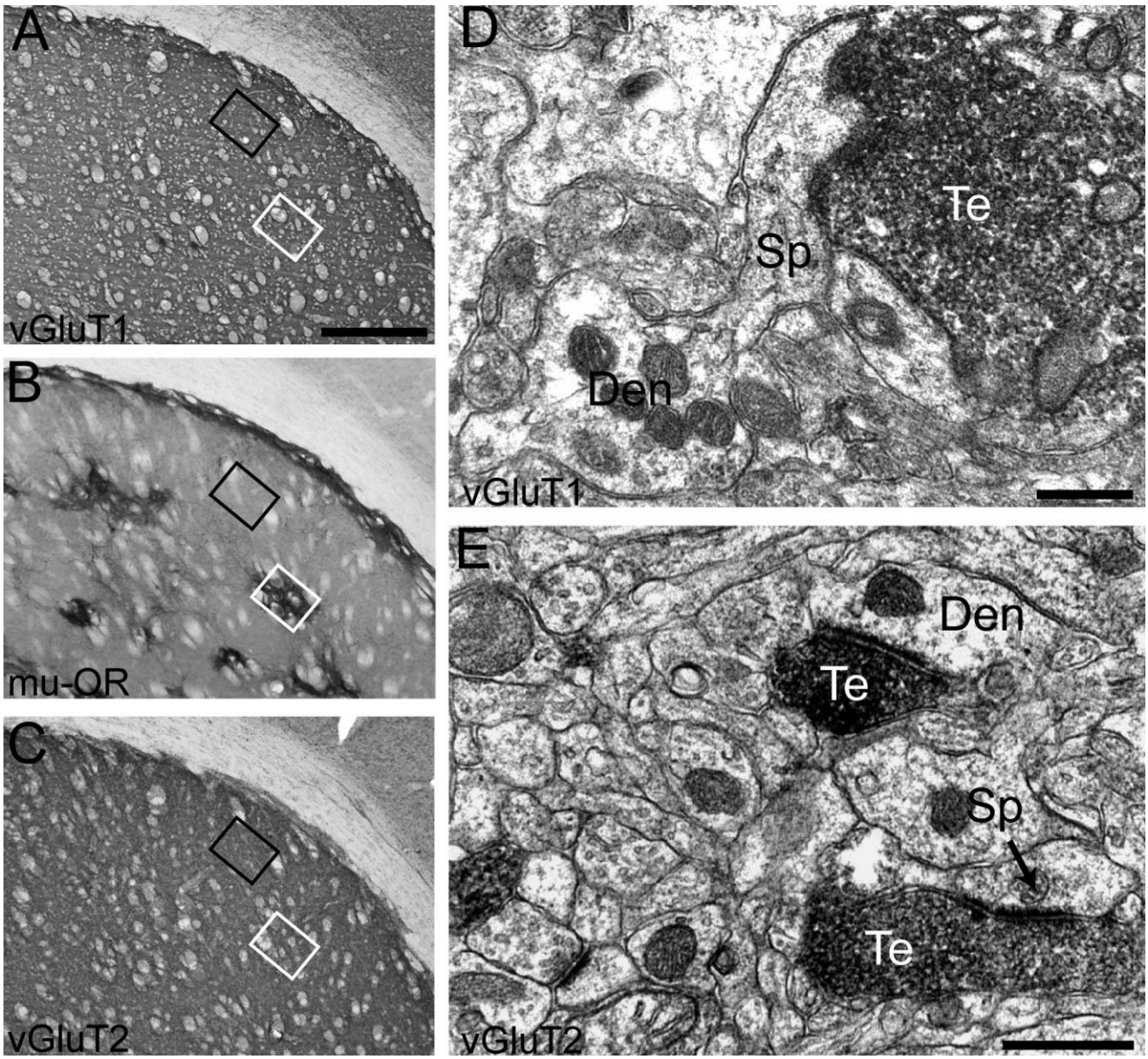

Fig. 2. Distribution of vGluT1- and vGluT2-immunolabeled axon terminals in the patch and matrix compartments. Patch and matrix compartments of the striatum were identified by immunostaining for μ-OR at the light microscopic level (**B**). Sections immediately preceding and after that stained for μ-OR were incubated with vGluT1 or vGluT2 antibodies and processed for electron microscopic observation. Immunostaining for vGluT1 (**A**) and vGluT2 (**C**) at the light microscopic level is shown here to illustrate how blocks of tissue from the patch and matrix were obtained. Sections stained for vGluT1, μ-OR, and vGluT2 were placed side by side, and areas corresponding to the patch (white boxes) and matrix (black boxes) in the μ-OR-immunostained section were cut out form the vGluT1- and vGluT2-immunolabeled sections. At the electron microscopic level, vGluT1 and vGluT2 immunoreactivity was restricted primarily to axon terminals (**D,E**) forming asymmetric synapses (arrow in E). Te, terminals; Den, dendrite; Sp, spine. Scale bars = 500 μm in A (applies to A–C); 0.5 μm in D,E.

The core of all thalamic PHA-L injections contained densely labeled neuronal cell bodies that were confined to the injected nuclei (Fig. 4A1–H1). Injections of the primary motor cortex (Fig. 4A1) and PF (Fig. 4B1) were restricted entirely within these structures, whereas injections involving the CL showed slight contamination of the medial LD and dorsal VL (Fig. 4C1). The cores of midline injections were centered in the IMD but encompassed the PV and CeM (Fig. 4D1), with negligible spillover to the PC. MD injection sites were centered within this nucleus but showed slight contamination of the neighboring CL and PC (Fig. 4E1). PHA-L delivery to the LD was restricted to the medial division of the nucleus, with minimal contamination of the Po (Fig. 4F1). Injections targeting the AV resulted in some spillover to the RT and dorsal AM (Fig. 4G1). PHA-L deposits were restricted to the

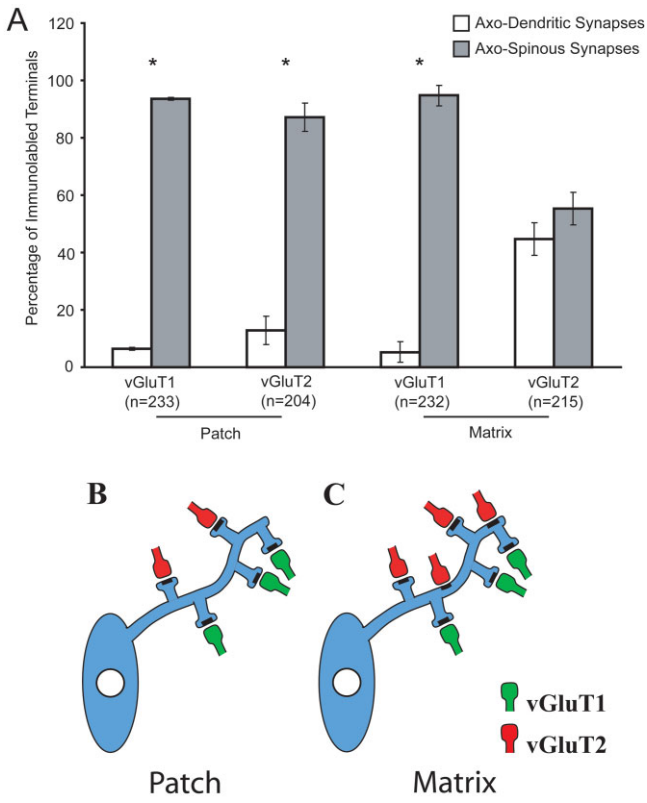

Fig. 3. Differential synaptology of vGluT1- and vGluT2-labeled terminals in the patch and matrix compartments. VGluT1-positive terminals within the patch and matrix and vGluT2-positive terminals within the matrix formed significantly more axospinous synapses than axodendritic synapses (*$P < 0.05$), whereas vGluT2-positive terminals within the matrix compartment contacted dendritic shafts and spines at similar proportions (**A**). The differential synaptic innervation patterns of vGluT1- and vGluT2-labeled terminals in the compartments are summarized (**B,C** n = number of terminals). Error bars show SEM.

VA/VL, with negligible spread to the VPL. Anterogradely labeled fibers in the striatum from the injected nuclei formed a dense plexus with varying degrees of terminal specializations and varicosities (Fig. 4A2–H2). Projections from the M1, PF, and CL targeted the dorsolateral striatum (Fig. 4A2–C2), whereas projections from the midline nuclei terminated in the ventral striatum (Fig. 4D2). Afferents from the MD were found in the medial part of the dorsal striatum, near the lateral ventricle and in the ventral striatum (Fig. 3E1). Anterogradely labeled neuronal fibers from the LD and VA/VL terminated in the dorsal edge and dorsocentral striatum (Fig. 4F2,H2), and projections from the AV terminated along the dorsomedial border of the striatum (Fig. 4G2). Overall, the pattern of distribution of anterograde labeling in the striatum was consistent with that described in previous studies (Dube et al., 1988; Groenewegen, 1988; Berendse and Groenewegen, 1990; Pinto et al., 2003; Smith et al., 2004; Fig. 4A2–H2).

Blocks of tissue from the densest areas of striatal labeling following these injections were selected and examined in the electron microscope (Table 2). In all cases, PHA-L-immunolabeled axon terminals contained round synaptic vesicles and zero to three mitochondria and formed exclusively asymmetric synapses with dendritic spines or shafts (Fig. 4A3–H3).

Several previous studies in rats and monkeys have examined the synaptology of afferents from the M1 and PF (Dube et al., 1988; Meredith and Wouterlood, 1990; Lapper and Bolam, 1992; Sadikot et al., 1992b), showing that the majority of M1 afferents innervate dendritic spines, whereas most PF projections terminate onto dendritic shafts in the striatum. In line with these findings, over 90% of M1 corticostriatal afferents formed axospinous synapses, whereas 89% of PF terminals contacted dendritic shafts in our study (Fig. 5). However, in striking contrast to the thalamic inputs from PF, all other thalamic inputs examined from CL (99%), MD (96%), LD (93%), AV (100%), VA/VL (99%), and midline (98%) thalamic nuclei formed axospinous synapse in the rat striatum (Fig. 5).

DISCUSSION

This study provides the first detailed analysis of the synaptology of a large sample of individual thalamic nuclei to the rat striatum. The following conclusions can be drawn from these observations: First, corticostriatal afferents, identified by vGluT1 immunolabeling (Fremeau et al., 2004; Smith et al., 2004), form preferentially axospinous synapses irrespective of the striatal compartment in which they terminate. In contrast, thalamostriatal afferents, identified by vGluT2 immunolabeling (Fremeau et al., 2004; Smith et al., 2004; Hur and Zaborszky, 2005), differentially innervate the patch and matrix compartments. VGluT2-containing boutons in patches terminate almost exclusively onto dendritic spines, whereas vGluT2 innervation of the matrix is equally distributed onto dendritic spines and shafts of striatal neurons. Second, thalamostriatal afferents from various relay (MD and VA/VL), associative (AV and LD), rostral intralaminar (CL), and midline (PV/IMD) thalamic nuclei form axospinous synapses, much like corticostriatal afferents. In contrast, striatal inputs from the caudal intralaminar nucleus, the PF, almost exclusively innervate dendritic shafts (Dube et al., 1988; Lapper and Bolam, 1992). Together, these findings provide further evidence for the high degree of synaptic specificity of the thalamostriatal system (Groenewegen and Berendse, 1984; Smith et al., 2004) and highlight the unique feature of PF inputs to the striatum compared with other thalamostriatal systems.

Vesicular glutamate transporters are selective markers of corticostriatal and thalamostriatal synapses

Several lines of evidence support the idea that vGluT1 is a selective marker for corticostriatal afferents, whereas vGluT2 identifies thalamostriatal projections. First, in situ hybridization studies for vGluT1 and vGluT2 mRNA have shown that neurons in all layers of the neocortex express vGluT1, whereas layers IV of the frontal and parietal cortices and layers IV and VI of the temporal cortex contain vGluT2 (Hisano et al., 2000; Fremeau et al., 2001, 2004). Because most corticostriatal afferents arise from layers III and V (Charara et al., 2002), it is highly likely that corticostriatal afferents utilize vGluT1. On the other hand, the thalamus expresses substantially more

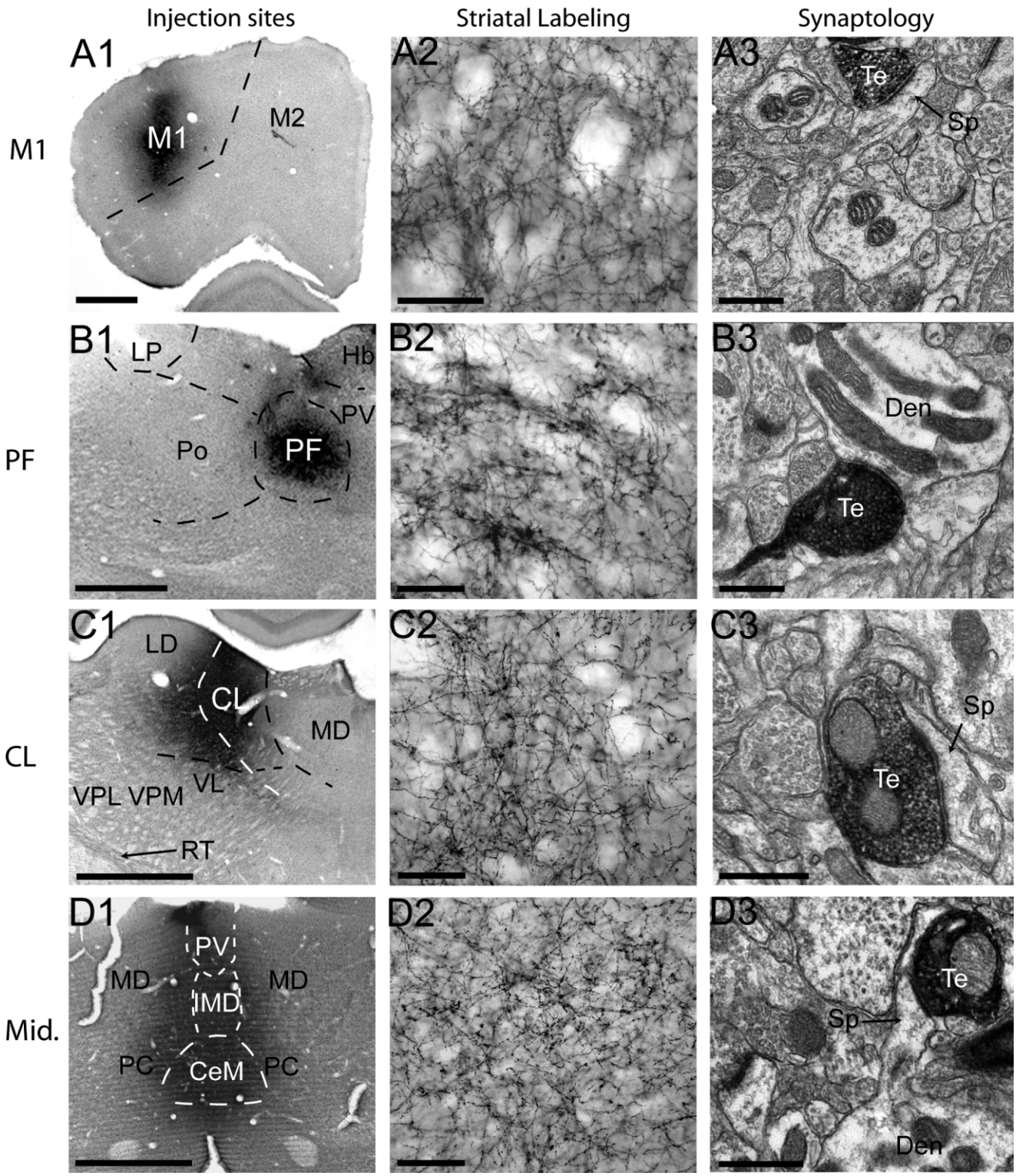

Fig. 4. Injection sites, striatal labeling and synaptology of corticostriatal and thalamostriatal afferents. Injection sites are shown in **A1–H1**. Dashed lines delineate the approximate boundaries of specific thalamic nuclei. Injections of the primary motor cortex (A1) and PF (B1) are restricted entirely within these structures, whereas injections involving the CL showed slight contamination of the medial LD and dorsal VL (C1). The core of midline injections was centered in the IMD but encompassed the PV and CeM (D1), with negligible spillover to the PC. MD injection sites were centered within this nucleus but showed slight contamination of the neighboring CL and PC (E1). PHA-L delivery to the LD was restricted to the medial division of the nucleus, with minimal contamination of the Po (F1). Injections targeting the AV resulted in some spillover to the RT and dorsal AM (G1). PHA-L deposits were restricted to the VA/VL, with negligible spread to the VPL. Anterogradely labeled fibers in the striatum from the injected nuclei formed a dense plexus with varying degrees of terminal specializations and varicosities (**A2–H2**). The synaptology of anterogradely labeled axon terminals is shown in **A3–H3**. All axon terminals examined formed asymmetric synapses and in all cases, except that of the PF, are shown terminating onto dendritic spines. Projections from the M1, midline nuclei, and LD can be seen terminating onto spines extending from the parent dendrite (A3,D3,F3). Axon terminals arising form the PF contacts a dendrite. Te, terminals; Den, dendrite; Sp, spine. Scale bars = 500 μm in A1–H3; 200 μm in A2–H2; 0.5 μm in A3–H3.

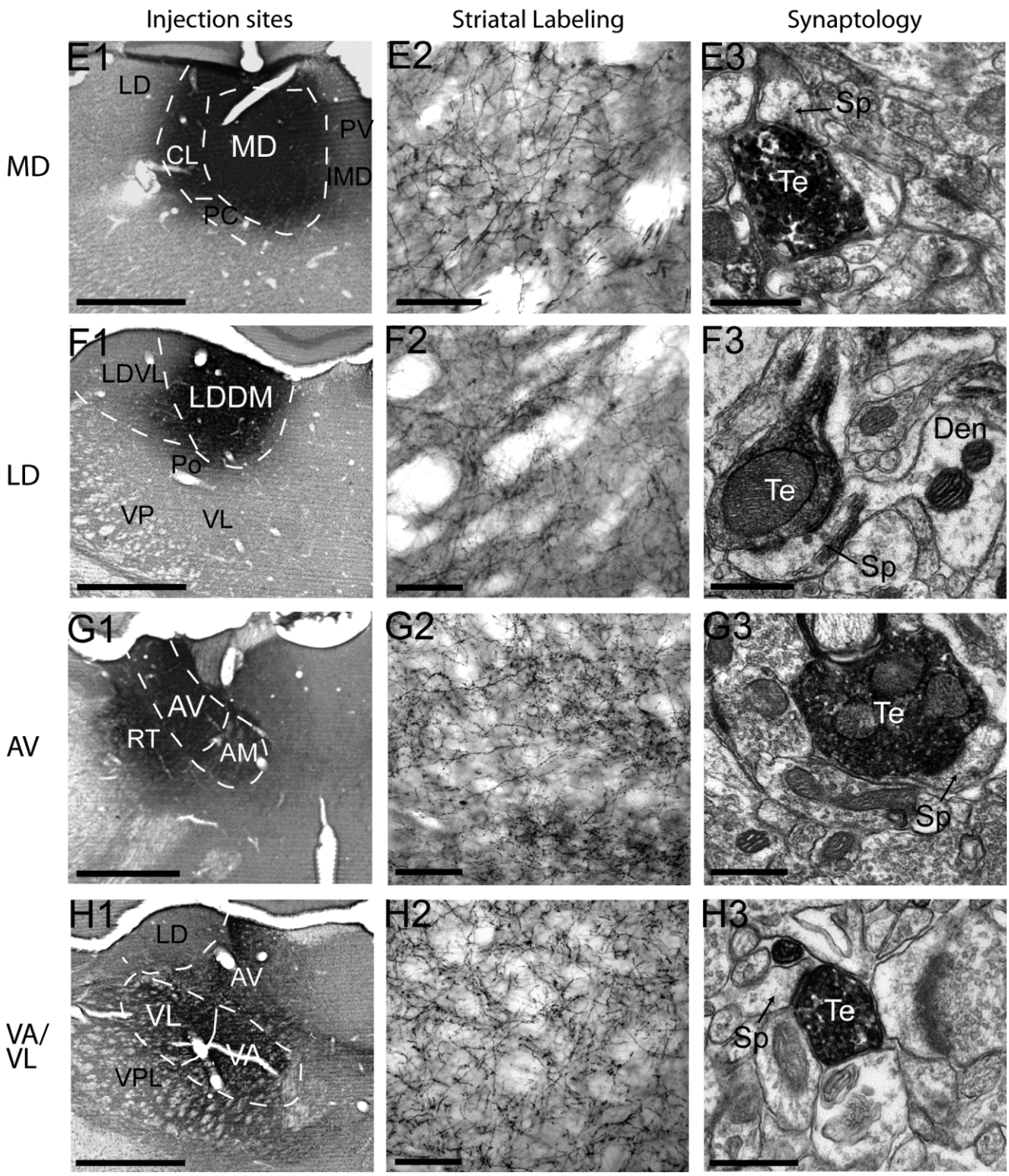

Figure 4 (Continued)

vGluT2 than vGluT1 mRNA (Fremeau et al., 2001, 2004). Second, in situ hybridization for vGluT2 mRNA combined with retrograde labeling of the medial prefrontal cortex identified a large population of doubly labeled thalamocortical neurons in the intralaminar, midline, and mediodorsal nuclei, whereas injections of retrograde tracer in the

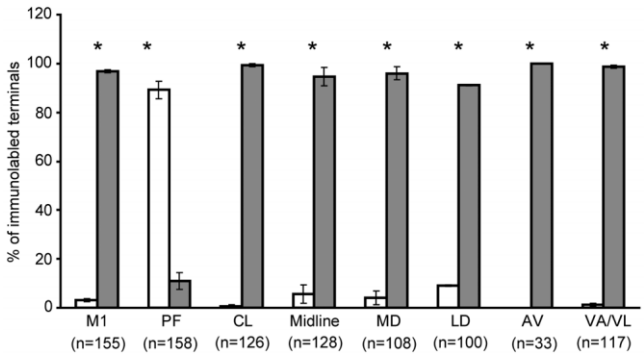

Fig. 5. Postsynaptic targets of corticostriatal and thalamostriatal afferents. Afferents from M1 and all thalamic nuclei examined, except for the PF, formed significantly more axospinous synapses than axodendritic synapses (*$P < 0.05$), whereas axon terminals arising from the PF preferentially innervated dendritic shafts (*$P < 0.05$). Excluding the PF, the percentage of terminals from various thalamic nuclei forming axospinous synapses did not differ significantly from corticostriatal afferents ($P > 0.05$). These data were gathered from the examination of both patch and matrix compartments (n = number of terminals). Error bars show SEM.

primary somatosensory cortex and the neighboring posterior parietal cortex identified thalamocortical neurons within the VL, AV, and LD. Most importantly, almost 99% of the retrogradely labeled thalamocortical neurons expressed vGluT2 mRNA, indicating that the thalamus uses vGluT2 (Hur and Zaborszky, 2005). Third, confocal microscopic examination of vGluT1 and vGluT2 proteins in the rat striatum revealed a complete segregation of these two transporters in striatal terminals (Fujiyama et al., 2004; Lacey et al., 2005). Fourth, lesions of the intralaminar thalamic nuclei significantly reduced vGluT2 expression in the striatum (Bacci et al., 2004). Finally, electron microscopic studies of vGluT1 and vGluT2 proteins in the rat striatum showed that less than 1.5% of immunolabeled terminals were doubly labeled for both transporters (Raju and Smith, 2005). Together, these results provide strong evidence that vGluT1 and vGluT2 are used by corticofugal and thalamofugal neurons, respectively.

The primary sources of glutamatergic innervation to the dorsal striatum arise from the cortex and thalamus. In rat, the basolateral amygdala, which primarily expresses vGluT1 mRNA, is another source of glutamatergic afferents to both the dorsal and the ventral striatum (Kita and Kitai, 1990; Fremeau et al., 2001). Amygdalostriatal afferents target almost exclusively dendritic spines in the matrix compartment (Kita and Kitai, 1990). Therefore, although vGluT1 immunolabeling identifies axon terminals from the basolateral amygdala and the cortex, the fact that both inputs form axospinous synapses makes us confident that this dual source of vGluT1-containing terminals should not be a problem for the interpretation of data presented in this study. Also, it is noteworthy that the neocortex is the overwhelming primary source of axon terminals forming asymmetric synapses within the striatum (Parent and Hazrati, 1995; Ingham et al., 1998; Kincaid et al., 1998), suggesting that the vGluT1-immunolabeled axon terminals are primarily of neocortical origin.

Differential distribution of vGluT1 and vGluT2 within the patch and matrix compartments

Because thalamostriatal afferents from the caudal intralaminar nuclei innervate preferentially the matrix and form predominantly axodendritic synapses, we examined the possibility that vGluT2-immunolabeled axon terminals preferentially innervate dendritic shafts within the matrix compared with the patch compartments. Our findings demonstrate that the intrastriatal synaptic connectivity of vGluT2-containing terminals is more heterogeneous than that of vGluT1-immunoreactive boutons and differs between the patch and the matrix compartments. In the patch, the majority of vGluT2-containing terminals contacted dendritic spines, whereas, in the matrix, immunoreactive boutons were distributed more evenly between axodendritic and axospinous synapses. These data provide the first evidence for a differential synaptic organization of glutamatergic afferents to the patch and matrix compartments (Fig. 3). It is noteworthy that the synaptology of nigrostriatal terminals does not differ between patches and matrix compartments (Hanley and Bolam, 1997), which highlights the specificity of the changes described in this study for vGluT2-containing thalamic terminals.

Striatal afferents from most intralaminar and midline nuclei, except the PV and rhomboid, terminate primarily in the matrix compartment of the ventral striatum (Berendse and Groenewegen, 1990), whereas projections from the caudal intralaminar as well as the VA/VL, AV, and LD innervate preferentially the matrix compartment of the dorsal striatum (Herkenham and Pert, 1981; Ragsdale and Graybiel, 1991; Sadikot et al., 1992b). Because of the preponderance of thalamic inputs to the matrix compartment, the potential source of thalamic innervation of the patch compartment remains to be determined. Although the absolute number of vGluT2-positive terminals in the patch and matrix compartments was not determined in the present study, it is possible that thalamic projections to the patch compartment are sparser than to the matrix. Two potential sources of thalamostriatal afferents to the patch compartment of the dorsal striatum are the CL and MD, two thalamic nuclei that project to the dorsal striatum and are reciprocally connected with limbic cortices (Gerfen, 1984; Groenewegen, 1988; Van der Werf et al., 2002). Because limbic and associative cortices preferentially innervate the patch compartment (Eblen and Graybiel, 1995; Wang and Pickel, 1998), the CL and MD are likely candidates for the thalamic innervation of the patch, but this remains to be tested using selective markers of the patch and matrix combined with anterograde labeling of striatal inputs from these nuclei.

Synaptology of thalamostriatal afferents

To test the hypothesis that thalamostriatal projections, other than those from the PF, preferentially target dendritic spines, we examined the synaptology of axon terminals from various thalamic nuclei within the striatum, by using anterograde tract tracing methods. In all examined cases, thalamic afferents, except those from the PF, preferentially innervated dendritic spines. These results strongly indicate that the vGluT2 innervation of the matrix is a composite of PF afferents forming axodendritic synapses and all other thalamic nuclei under study forming axospinous synapses; which is consistent with previ-

ous tract-tracing studies in rodents (Xu et al., 1991; Ichinoe et al., 2001; Pinto et al., 2003; Smith et al., 2004). Although the relative contribution of individual thalamic nuclei to the thalamostriatal system was not determined, the near equal innervation onto dendritic spines and shafts by vGluT2-positive boutons suggests that about half of the thalamic innervation to the matrix originates from the PF. These results demonstrate that the PF is a unique source of thalamic inputs that target preferentially dendritic shafts in the striatum (Fig. 5).

Two major targets of PF are the medium spiny projection neurons and cholinergic interneurons (Meredith and Wouterlood, 1990; Lapper and Bolam, 1992; Sidibe and Smith, 1999; Smith et al., 2004). In monkeys, projections from the centromedian (CM) nucleus innervate preferentially striatofugal cells projecting to the internal pallidum, suggesting that caudal intralaminar nuclei provide positive feedback to the so-called direct pathway (Sidibe and Smith, 1996). In addition, striatal afferents from the caudal intralaminar thalamic nuclei target cholinergic interneurons (Sidibe and Smith, 1999; Smith et al., 2004), which, in turn, target medium spiny neurons (Izzo and Bolam, 1988). Because striatal interneurons lack dendritic spines, our findings suggest that most thalamic nuclei, other than CM/PF, are unlikely to innervate interneurons to a significant degree. In fact, examination of intrastriatal connectivity of afferents from the CL in rat showed no significant innervation of parvalbumin-containing interneurons (Ichinohe et al., 2001), whereas thalamostriatal afferents from the CM/PF in monkeys, but not in rats, contact this class of interneurons (Rudkin and Sadikot, 1999; Sidibe and Smith, 1999). Although one cannot completely rule out the possibility that a small fraction of thalamic inputs to striatal interneurons arises from relay or rostral intralaminar thalamic nuclei, it is very likely that the bulk of thalamic innervation to these neurons originates from the CM/PF. This provides further evidence for the high degree of heterogeneity and specificity of the thalamostriatal system (Smith et al., 2004).

A key feature of the corticostriatal innervation is its tight relationship with dopaminergic axon terminals. In rats, corticostriatal and nigrostriatal afferents frequently converge onto individual dendritic spines, the cortical inputs being in contact with the spine head, whereas the dopaminergic inputs terminate preferentially onto the spine neck (Smith and Bolam, 1990). In monkeys, corticostriatal afferents from the primary motor and somatosensory cortices were found to converge with tyrosine hydroxylase-positive axon terminals on the same dendritic spines (Smith et al., 1994). This synaptic arrangement is considered as the main anatomical substrate by which dopaminergic inputs modulate cortical information flow in the striatum. On the other hand, thalamic afferents from the CM/PF, because of their preferential innervation of dendritic shafts, may be precluded from having potential interactions with nearby dopaminergic synapses (Smith et al., 1994). However, the findings of the present study suggest that most thalamic inputs, except those from CM/PF, could be modulated by dopaminergic afferents at the level of individual spines. Given the important modulatory role dopamine plays in regulating glutamatergic transmission and striatal processing (Nicola et al., 2000; Bamford et al., 2004), a detailed analysis of the degree of synaptic convergence of thalamic and dopaminergic inputs onto single spines is warranted to address this issue further. In that regard, it is noteworthy that thalamic inputs from the paraventricular nucleus were found to be closely apposed to TH-immunopositive axon terminals, and, in some cases, both types of terminals formed synapses onto the same dendritic spine in rats (Pinto et al., 2003).

Functional implications

Findings presented in this study demonstrate the unique features that characterize the synaptology of thalamostriatal projections form the PF compared with other thalamic inputs to the rat striatum. Other anatomical and functional characteristics could be considered as evidence that the CM/PF complex displays unique relationships with the basal ganglia. Several lines of evidence suggest that the primary target of the CM/PF is the striatum rather than the neocortex. For example, in the monkey, the lateral one-third of the CM contains thalamocortical neurons, whereas the medial CM and PF project preferentially to the so-called sensorimotor and associative striatum, respectively (Fenelon et al., 1991; Francois et al., 1991; Sadikot et al., 1992a; Parent and Hazrati, 1995; Smith et al., 2004). Furthermore, single-cell filling studies in rat and monkey have shown that thalamostriatal axons from the PF arborize extensively within the striatum but only sparsely within the neocortex (Deschenes et al., 1996a). In striking contrast to the caudal intralaminar thalamic nuclei, projections from the CL arborize heavily within the neocortex, establishing larger terminal fields, compared with sparse collaterals directed to the striatum, which form en passant synapses (Deschenes et al., 1996b). Similar studies in the VA/VL reveal that neurons target primarily sensorimotor cortices in rat (Aumann et al., 1998). Moreover, retrograde labeling studies in cat identified that thalamocortical neurons of the relay and rostral intralaminar nuclei also project to the caudate nucleus, whereas those from the caudal intralaminar complex terminate preferentially in the caudate nucleus (Royce, 1978). Such differences in projections to the striatum and neocortex between caudal intralaminar and rostral intralaminar and relay thalamic nuclei suggest that the PF is dedicated toward information processing within the basal ganglia, whereas other thalamic nuclei are involved in carrying information to the neocortex. The differential innervation of PF inputs onto dendritic shafts of medium spiny neurons, compared with all other thalamic nuclei examined, adds another unique feature to this particular projection that may affect its role in the functional integration of the synaptic microcircuitry of striatal medium spiny neurons (Smith and Bolam, 1990; Wilson, 1995; Smith et al., 2004).

Changes in the relative size of the patch and matrix compartments have been reported for several neurodegenerative diseases. For example, the putamen of patients with motor neuron diseases and basophilic inclusions shows a selective loss of patches (Ito et al., 1995). Similarly, the caudate nucleus and putamen of patients with X-linked recessive dystonia-parkinsonism exhibits increasing degeneration of the patch compartment, with progression of the disease (Goto et al., 2005). In monkeys treated with the neurotoxin 1-methyl-4-phenyl-1,2,3,6-tetrahydropyridine, 5-HT1A serotonin receptors are increased (Frechilla et al., 2001), whereas dopamine binding sites are maintained in the patch compared with the matrix compartment (Moratalla et al., 1992). Furthermore,

activation of dopamine receptors in rats causes an increase in repetitive motor behaviors. These motor stereotypies are directly correlated with increased immediate early gene expression in the patches compared with the matrix (Canales and Graybiel, 2000). These results strongly suggest that a balance of activity between the patch and the matrix compartments regulates normal basal ganglia function and that an imbalance toward a specific compartment may lead to striatal dysfunction. Thus, a shift in the differential innervation of thalamic inputs to areas within the patch and matrix compartments may lead to significant changes in striatal activity and might thereby underlie abnormal regulation of basal ganglia activity in disease states.

ACKNOWLEDGMENTS

The authors thank Jean-Francois Pare and Susan Maxson for technical assistance and also Mr. Craig Heilman (Mab Technologies) for the generous gift of vGluT1 antibodies.

LITERATURE CITED

Aumann TD, Ivanusic J, Horne MK. 1998. Arborisation and termination of single motor thalamocortical axons in the rat. J Comp Neurol 396:121–130.

Bacci JJ, Kachidian P, Kerkerian-Le Goff L, Salin P. 2004. Intralaminar thalamic nuclei lesions: widespread impact on dopamine denervation-mediated cellular defects in the rat basal ganglia. J Neuropathol Exp Neurol 63:20–31.

Bamford NS, Robinson S, Palmiter RD, Joyce JA, Moore C, Meshul CK. 2004. Dopamine modulates release from corticostriatal terminals. J Neurosci 24:9541–9552.

Berendse HW, Groenewegen HJ. 1990. Organization of the thalamostriatal projections in the rat, with special emphasis on the ventral striatum. J Comp Neurol 299:187–228.

Canales JJ, Graybiel AM. 2000. A measure of striatal function predicts motor stereotypy. Nat Neurosci 3:377–383.

Charara A, Sidibe M, Smith Y. 2002. Basal ganglia circuitry and synaptic connectivity. In: Tarsy D, Vitek JL, Lozano AM, editors. Surgical treatment of Parkinson's disease and other movement disorders. Totowa, NJ: Humana Press. p 19–39.

Desban M, Gauchy C, Kemel ML, Besson MJ, Glowinski J. 1989. Three-dimensional organization of the striosomal compartment and patchy distribution of striatonigral projections in the matrix of the cat caudate nucleus. Neuroscience 29:551–566.

Desban M, Kemel ML, Glowinski J, Gauchy C. 1993. Spatial organization of patch and matrix compartments in the rat striatum. Neuroscience 57:661–671.

Deschenes M, Bourassa J, Doan VD, Parent A. 1996a. A single-cell study of the axonal projections arising from the posterior intralaminar thalamic nuclei in the rat. Eur J Neurosci 8:329–343.

Deschenes M, Bourassa J, Parent A. 1996b. Striatal and cortical projections of single neurons from the central lateral thalamic nucleus in the rat. Neuroscience 72:679–687.

Dube L, Smith AD, Bolam JP. 1988. Identification of synaptic terminals of thalamic or cortical origin in contact with distinct medium-size spiny neurons in the rat neostriatum. J Comp Neurol 267:455–471.

Eblen F, Graybiel AM. 1995. Highly restricted origin of prefrontal cortical inputs to striosomes in the macaque monkey. J Neurosci 15:5999–6013.

Fenelon G, Francois C, Percheron G, Yelnik J. 1991. Topographic distribution of the neurons of the central complex (centre median-parafascicular complex) and of other thalamic neurons projecting to the striatum in macaques. Neuroscience 45:495–510.

Francois C, Percheron G, Parent A, Sadikot AF, Fenelon G, Yelnik J. 1991. Topography of the projection from the central complex of the thalamus to the sensorimotor striatal territory in monkeys. J Comp Neurol 305:17–34.

Frechilla D, Cobreros A, Saldise L, Moratalla R, Insausti R, Luquin M, Del Rio J. 2001. Serotonin 5-HT(1A) receptor expression is selectively enhanced in the striosomal compartment of chronic parkinsonian monkeys. Synapse 39:288–296.

Fremeau RT Jr, Troyer MD, Pahner I, Nygaard GO, Tran CH, Reimer RJ, Bellocchio EE, Fortin D, Storm-Mathisen J, Edwards RH. 2001. The expression of vesicular glutamate transporters defines two classes of excitatory synapse. Neuron 31:247–260.

Fremeau RT Jr, Voglmaier S, Seal RP, Edwards RH. 2004. VGLUTs define subsets of excitatory neurons and suggest novel roles for glutamate. Trends Neurosci 27:98–103.

Fujiyama F, Kuramoto E, Okamoto K, Hioki H, Furuta T, Zhou L, Nomura S, Kaneko T. 2004. Presynaptic localization of an AMPA-type glutamate receptor in corticostriatal and thalamostriatal axon terminals. Eur J Neurosci 20:3322–3330.

Gerfen CR. 1984. The neostriatal mosaic: compartmentalization of corticostriatal input and striatonigral output systems. Nature 311:461–464.

Gerfen CR. 1989. The neostriatal mosaic: striatal patch-matrix organization is related to cortical lamination. Science 246:385–388.

Gerfen CR. 1992. The neostriatal mosaic: multiple levels of compartmental organization. Trends Neurosci 15:133–139.

Goto S, Lee LV, Munoz EL, Tooyama I, Tamiya G, Makino S, Ando S, Dantes MB, Yamada K, Matsumoto S, Shimazu H, Kuratsu J, Hirano A, Kaji R. 2005. Functional anatomy of the basal ganglia in X-linked recessive dystonia-parkinsonism. Ann Neurol 58:7–17.

Graybiel AM, Ragsdale CW Jr, Yoneoka ES, Elde RP. 1981. An immunohistochemical study of enkephalins and other neuropeptides in the striatum of the cat with evidence that the opiate peptides are arranged to form mosaic patterns in register with the striosomal compartments visible by acetylcholinesterase staining. Neuroscience 6:377–397.

Groenewegen HJ. 1988. Organization of the afferent connections of the mediodorsal thalamic nucleus in the rat, related to the mediodorsal-prefrontal topography. Neuroscience 24:379–431.

Groenewegen HJ, Berendse HW. 1984. The specificity of the "nonspecific" midline and intralaminar thalamic nuclei. Trends Neurosci 17:52–57.

Hanley JJ, Bolam JP. 1997. Synaptology of the nigrostriatal projection in relation to the compartmental organization of the neostriataum in the rat. Neuroscience 81:353–370.

Herkenham M, Pert CB. 1981. Mosaic distribution of opiate receptors, parafascicular projections and acetylcholinesterase in rat striatum. Nature 291:415–418.

Hisano S, Hoshi K, Ikeda Y, Maruyama D, Kanemoto M, Ichijo H, Kojima I, Takeda J, Nogami H. 2000. Regional expression of a gene encoding a neuron-specific Na^+-dependent inorganic phosphate cotransporter (DNPI) in the rat forebrain. Brain Res Mol Brain Res 83:34–43.

Hsu SM, Raine L, Fanger H. 1981a. The use of antiavidin antibody and avidin-biotin-peroxidase complex in immunoperoxidase technics. Am J Clin Pathol 75:816–821.

Hsu SM, Raine L, Fanger H. 1981b. Use of avidin-biotin-peroxidase complex (ABC) in immunoperoxidase techniques: a comparison between ABC and unlabeled antibody (PAP) procedures. J Histochem Cytochem 29:577–580.

Hur EE, Zaborszky L. 2005. Vglut2 afferents to the medial prefrontal and primary somatosensory cortices: a combined retrograde tracing in situ hybridization. J Comp Neurol 483:351–373.

Ichinohe N, Iwatsuki H, Shoumura K. 2001. Intrastriatal targets of projection fibers from the central lateral nucleus of the rat thalamus. Neurosci Lett 302:105–108.

Ingham CA, Hood SH, Taggart P, Arbuthnott GW. 1998. Plasticity of synapses in the rat neostriatum after unilateral lesion of the nigrostriatal dopaminergic pathway. J Neurosci 18:4732–4743.

Ito H, Kusaka H, Matsumoto S, Imai T. 1995. Topographic involvement of the striatal efferents in basal ganglia of patients with adult-onset motor neuron disease with basophilic inclusions. Acta Neuropathol 89:513–518.

Izzo PN, Bolam JP. 1988. Cholinergic synaptic input to different parts of spiny striatonigral neurons in the rat. J Comp Neurol 269:219–234.

Kawaguchi Y. 1997. Neostriatal cell subtypes and their functional roles. Neurosci Res 27:1–8.

Kawaguchi Y, Wilson CJ, Emson PC. 1990. Projection subtypes of rat neostriatal matrix cells revealed by intracellular injection of biocytin. J Neurosci 10:3421–3438.

Kincaid AE, Zheng T, Wilson CJ. 1998. Connectivity and convergence of single corticostriatal axons. J Neurosci 18:4722–4731.

Kita H, Kitai ST. 1990. Amygdaloid projections to the frontal cortex and the striatum in the rat. J Comp Neurol 298:40–49.

Lacey CJ, Boyes J, Gerlach O, Chen L, Magill PJ, Bolam JP. 2005. $GABA_B$ receptors at glutamatergic synapses in the rat striatum. Neuroscience 136:1083–1095.

Lapper SR, Bolam JP. 1992. Input from the frontal cortex and the parafascicular nucleus to cholinergic interneurons in the dorsal striatum of the rat. Neuroscience 51:533–545.

Lapper SR, Smith Y, Sadikot AF, Parent A, Bolam JP. 1992. Cortical input to parvalbumin-immunoreactive neurones in the putamen of the squirrel monkey. Brain Res 580:215–224.

Meredith GE, Wouterlood FG. 1990. Hippocampal and midline thalamic fibers and terminals in relation to the choline acetyltransferase-immunoreactive neurons in nucleus accumbens of the rat: a light and electron microscopic study. J Comp Neurol 296:204–221.

Montana V, Ni Y, Sunjara V, Hua X, Parpura V. 2004. Vesicular glutamate transporter-dependent glutamate release from astrocytes. J Neurosci 24:2633–2642.

Moratalla R, Quinn B, DeLanney LE, Irwin I, Langston JW, Graybiel AM. 1992. Differential vulnerability of primate caudate-putamen and striosome-matrix dopamine systems to the neurotoxic effects of 1-methyl-4-phenyl-1,2,3,6-tetrahydropyridine. Proc Natl Acad Sci U S A 89:3859–3863.

Nicola SM, Surmeier J, Malenka RC. 2000. Dopaminergic modulation of neuronal excitability in the striatum and nuclus accumbens. Annu Rev Neurosci 23:185–215.

Parent A, Hazrati LN. 1995. Functional anatomy of the basal ganglia. I. The cortico-basal ganglia-thalamo-cortical loop. Brain Res Brain Res Rev 20:91–127.

Paxinos G, Watson C. 1998. The rat brain in stereotaxic coordinates. New York: Academic Press.

Peters A, Palay SL, Webster HF. 1991. The fine structure of the nervous system-neurons and their supporting cells, 3rd ed. New York: Oxford University Press.

Pinto A, Jankowski M, Sesack SR. 2003. Projections from the paraventricular nucleus of the thalamus to the rat prefrontal cortex and nucleus accumbens shell: ultrastructural characteristics and spatial relationships with dopamine afferents. J Comp Neurol 459:142–155.

Ragsdale CW Jr, Graybiel AM. 1981. The fronto-striatal projection in the cat and monkey and its relationship to inhomogeneities established by acetylcholinesterase histochemistry. Brain Res 208:259–266.

Ragsdale CW Jr, Graybiel AM. 1991. Compartmental organization of the thalamostriatal connection in the cat. J Comp Neurol 311:134–167.

Raju DV, Smith Y. 2005. Differential localization of vesicular glutamate transporters 1 and 2 in the rat striatum. In: Bolam JP, Ingham CA, Magill PJ, editors. The basal ganglia VIII. New York: Springer Science. p 601–610.

Reynolds ES. 1963. The use of lead citrate at high pH as an electron opaque stain in electron microscopy. J Cell Biol 17:208–212.

Royce GJ. 1978. Cells of origin of subcortical afferents to the caudate nucleus: a horseradish peroxidase study in the cat. Brain Res 153:465–475.

Rudkin TM, Sadikot AF. 1999. Thalamic input to parvalbumin-immunoreactive GABAergic interneurons: organization in normal striatum and effect of neonatal decortication. Neuroscience 88:1165–1175.

Sadikot AF, Parent A, Francois C. 1992a. Efferent connections of the centromedian and parafascicular thalamic nuclei in the squirrel monkey: a PHA-L study of subcortical projections. J Comp Neurol 315:137–159.

Sadikot AF, Parent A, Smith Y, Bolam JP. 1992b. Efferent connections of the centromedian and parafascicular thalamic nuclei in the squirrel monkey: a light and electron microscopic study of the thalamostriatal projection in relation to striatal heterogeneity. J Comp Neurol 320: 228–242.

Sidibe M, Smith Y. 1996. Differential synaptic innervation of striatofugal neurones projecting to the internal or external segments of the globus pallidus by thalamic afferents in the squirrel monkey. J Comp Neurol 365:445–465.

Sidibe M, Smith Y. 1999. Thalamic inputs to striatal interneurons in monkeys: synaptic organization and co-localization of calcium binding proteins. Neuroscience 89:1189–1208.

Smith AD, Bolam JP. 1990. The neural network of the basal ganglia as revealed by the study of synaptic connections of identified neurones. Trends Neurosci 13:259–265.

Smith Y, Bennett BD, Bolam JP, Parent A, Sadikot AF. 1994. Synaptic relationships between dopaminergic afferents and cortical or thalamic input in the sensorimotor territory of the striatum in monkey. J Comp Neurol 344:1–19.

Smith Y, Raju DV, Pare JF, Sidibe M. 2004. The thalamostriatal system: a highly specific network of the basal ganglia circuitry. Trends Neurosci 27:520–527.

Somogyi P, Bolam JP, Smith AD. 1981. Monosynaptic cortical input and local axon collaterals of identified striatonigral neurons. A light and electron microscopic study using the Golgi-peroxidase transport-degeneration procedure. J Comp Neurol 195:567–584.

Van der Werf YD, Witter MP, Groenewegen HJ. 2002. The intralaminar and midline nuclei of the thalamus. Anatomical and functional evidence for participation in processes of arousal and awareness. Brain Res Rev 39:107–140.

Wang H, Pickel VM. 1998. Dendritic spines containing mu-opioid receptors in rat striatal patches receive asymmetric synapses from prefrontal corticostriatal afferents. J Comp Neurol 396:223–237.

Wilson CJ. 1995. The contribution of cortical neurons to the firing pattern of striatal spiny neurons. In: Kouk JC, Davis JL, Beiser DG, editors. Models of information processing in the basal ganglia. Cambridge, MA: The MIT Press. p 29–50.

Xu ZC, Wilson CJ, Emson PC. 1991. Restoration of thalamostriatal projections in rat neostriatal grafts: an electron microscopic analysis. J Comp Neurol 303:22–34.